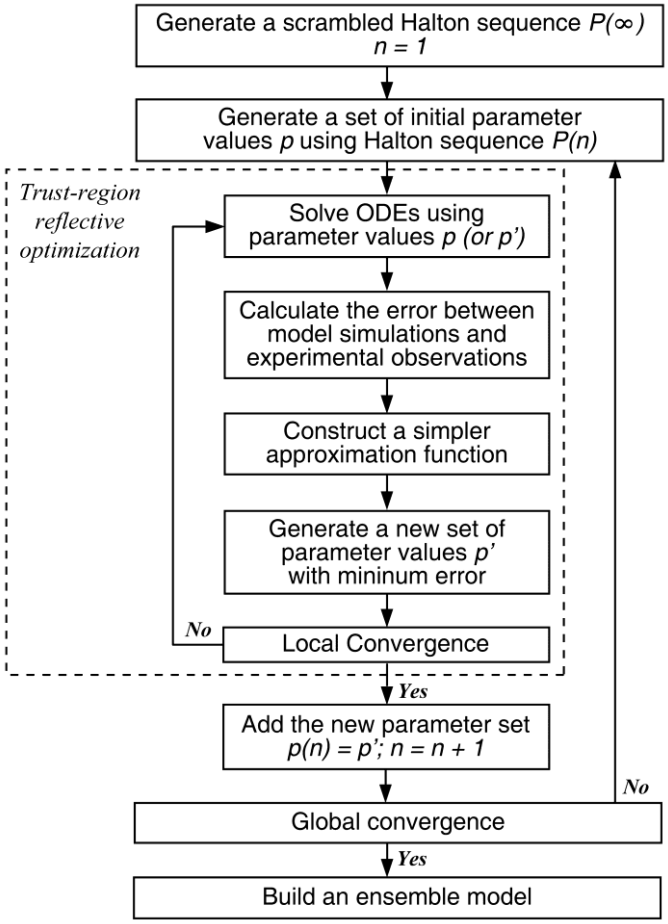

Fig. S1. Algorithm for HQEM. The steps of the HQEM algorithm is illustrated. The convergence is defined as the change in error is less than the specified tolerance, or the number of iterations exceeds the user specified maximum calculation steps.

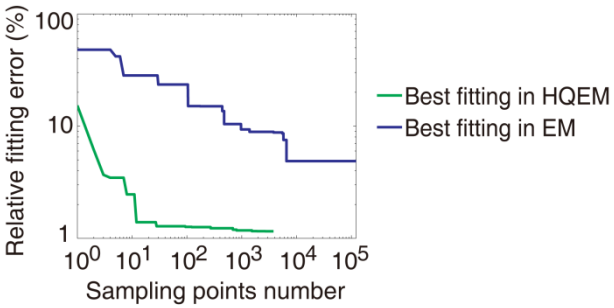

Fig. S2. Comparison of the optimization performance of hybrid quasi ensemble modeling (HQEM) and general ensemble modeling (EM). The relative fitting error of the best estimated parameter set, calculated by dividing the average error of all the sampling parameter sets, is plotted against the sampling points number.

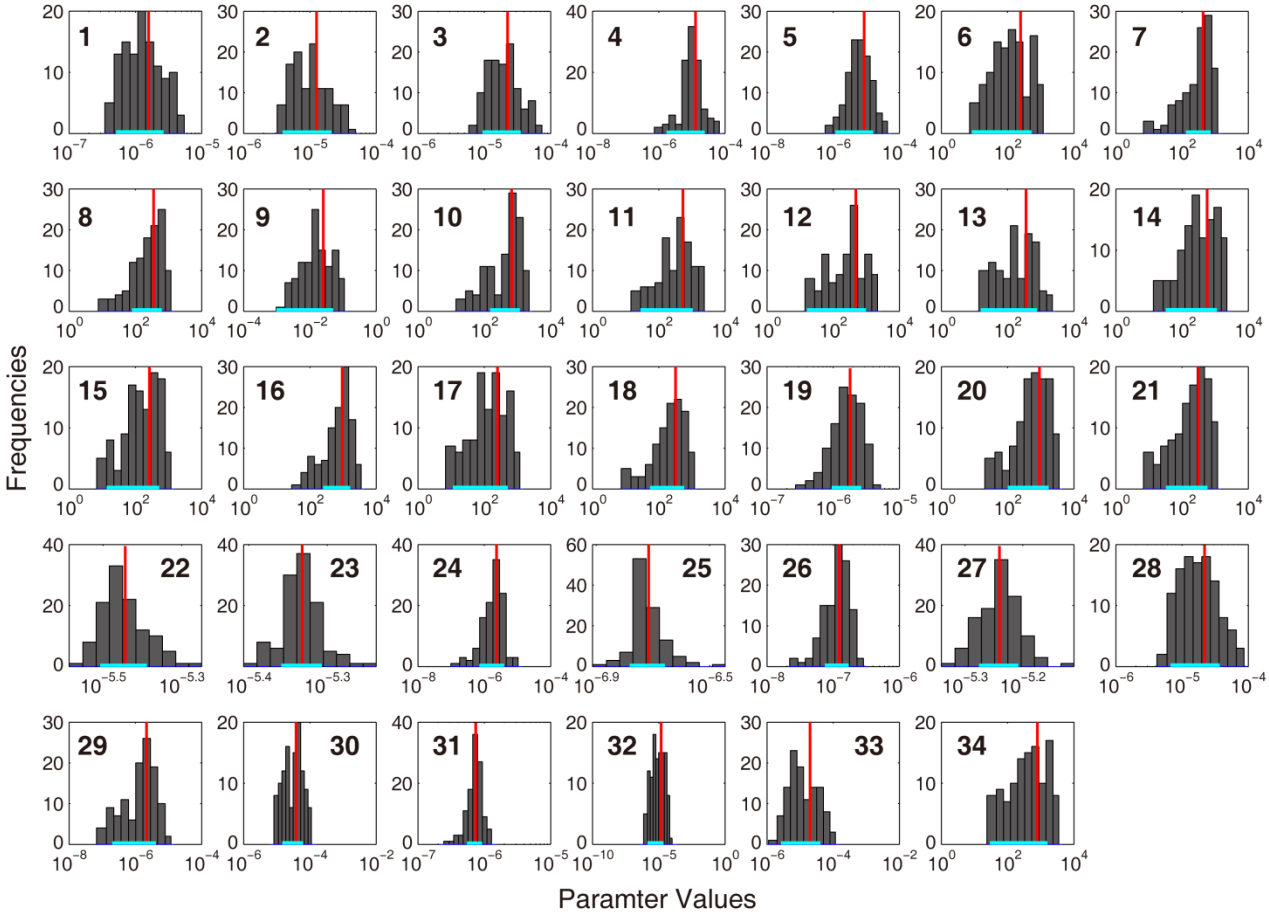

Fig. S3. Histogram plot of the values of 114 estimated ensemble parameter sets (34 parameters). The mean values for each parameter are marked in red lines (|). The standard deviations for each parameter are marked in cyan lines (—). The parameter names for parameter ID are as follows:

ID	Name	ID	Name	ID	Name
1	*kb_CyclinB_CDK1*	13	*kcat_AuroraAP_BoraPLK1*	25	*kb_AuroraAP_PLK1*
2	*kb_Wee1_CDK1B*	14	*kcat_AuroraAP_CDC25*	26	*kb_AuroraA_AuroraA*
3	*kb_CDC25_CDK1B*	15	*kcat_PLK1P_Wee1*	27	*kb_CDK1B_Wee1*
4	*kb_1433_CDC25*	16	*kcat_CDK1B_Wee1*	28	*kb_PLK1P_Bora*
5	*kb_CHK1_CDC25*	17	*kcat_CDC25_CDK1B*	29	*kb_PLK1P_CDC25*
6	*kcat_CHK1_CDC25*	18	*kcat_Wee1_CDK1B*	30	*kb_PLK1P_Claspin*
7	*kcat_PLK1P_Claspin*	19	*kb_CDK1B_CDC25*	31	*kb_PLK1P_Wee1*
8	*kcat_PLK1P_Bora*	20	*kcat_CDK1B_CDC25*	32	*kb_Claspin_CHK1*
9	*kb_Bora_PLK1*	21	*kcat_PLK1P_CDC25*	33	*kb_ATR_ClaspinCHK1*
10	*kcat_AuroraAP_PLK1*	22	*kb_AuroraAP_AuroraA*	34	*kcat_ATR_ClaspinCHK1*
11	*kcat_AuroraA_AuroraA*	23	*kb_AuroraAP_BoraPLK1*		
12	*kcat_AuroraAP_AuroraA*	24	*kb_AuroraAP_CDC25*		

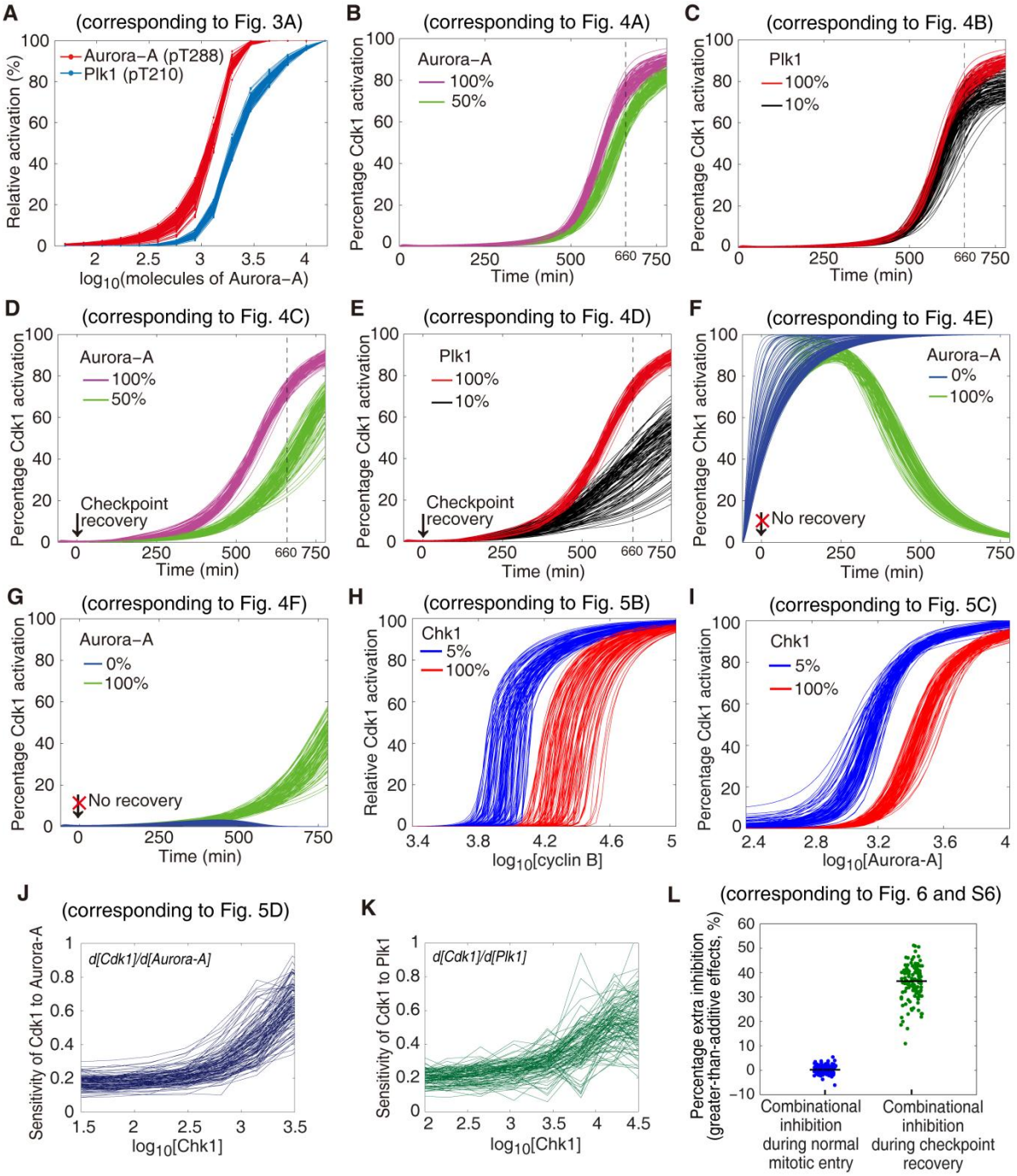

Fig. S4. Ensemble simulation results calculated based on the 114 parameter sets obtained by HQEM.

(A) Ensemble simulations of the influence of different amount of Aurora-A (*by altering the initial value of [AuroraA]*) to its own activation (*the amount of [AuroraA_pT288]*) and to the activation of Plk1 (*the amount of [PLK1_pT210]*) (corresponding to Fig. 3A).

(B,C) Ensemble simulated time courses of activated cyclin B/Cdk1 complex (*the amount of [CDK1_pT161:CyclinB]*) in response to different amount of (B) Aurora-A (*by altering the initial value of [AuroraA]*) and (C) Plk1 (*by altering the initial value of [PLK1]*) reveal the redundant function of Aurora-A and Plk1 during normal mitotic entry (corresponding to Fig. 4A, B).

(D,E) Ensemble simulated time courses of activated cyclin B/Cdk1 complex (*the amount of [CDK1_pT161:CyclinB]*) in response to different amount of (D) Aurora-A (*by altering the initial value of [AuroraA]*) and (E) Plk1 (*by altering the initial value of [PLK1]*) demonstrate the crucial functions of Aurora-A and Plk1 during checkpoint recovery (corresponding to Fig. 4C, D).

(F,G) Ensemble simulations of inappropriate hyperactive Aurora-A (*by altering the initial value of [AuroraA]*) promoting (F) the abnormal deactivation of Chk1 (*the amount of [CHK1_pS]*) and (G) the abnormal activation of cyclin B/Cdk1 (*the amount of [CDK1_pT161:CyclinB]*) even in the presence of G2/M checkpoint arrest signaling (corresponding to Fig. 4E, F).

(H,I) Ensemble simulations of the response of activated cyclin B/Cdk1 (*the amount of [CDK1_pT161:CyclinB]*) to the amount of (H) cyclin B (*by varying the initial value of [CycinB]*) and (I) Aurora-A (*by varying the initial value of [AuroraA]*) by altering the amount of Chk1 (*by altering the initial value of [Chk1]*) show that the threshold for cyclin B/Cdk1 activation is up-regulated in response to DNA-damage signaling (corresponding to Fig. 5B, C).

(J,K) The sensitivity of cyclin B/Cdk1 activation to changes in the amount of (J) Aurora-A and (K) Plk1 is up-regulated in response to Chk1 activation (corresponding to Fig. 5D).

(L) Ensemble simulation of the extra inhibition by concurrently targeting Aurora-A and Plk1 during normal mitotic entry and during checkpoint recovery (corresponding to Fig. 6, S6).

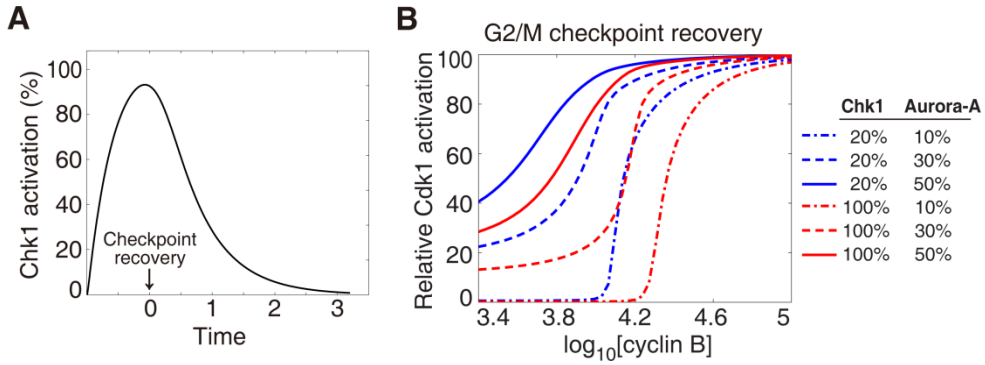

Fig. S5. (A) Simulation of the activation of Chk1 (*the amount of [CHK1]*) in response to DNA damage signaling, and its inactivation during G2/M checkpoint recovery. **(B)** Simulation of the relationship between the activities of cyclin B/Cdk1 (*the amount of [CDK1_pT161:CyclinB]*) and the concentrations of cyclin B (*by varying the initial value of [CycinB]*) in response to alterations of Chk1 (*by altering the initial value of [Chk1]*) and Aurora-A (*by altering the initial value of [AuroraA]*).

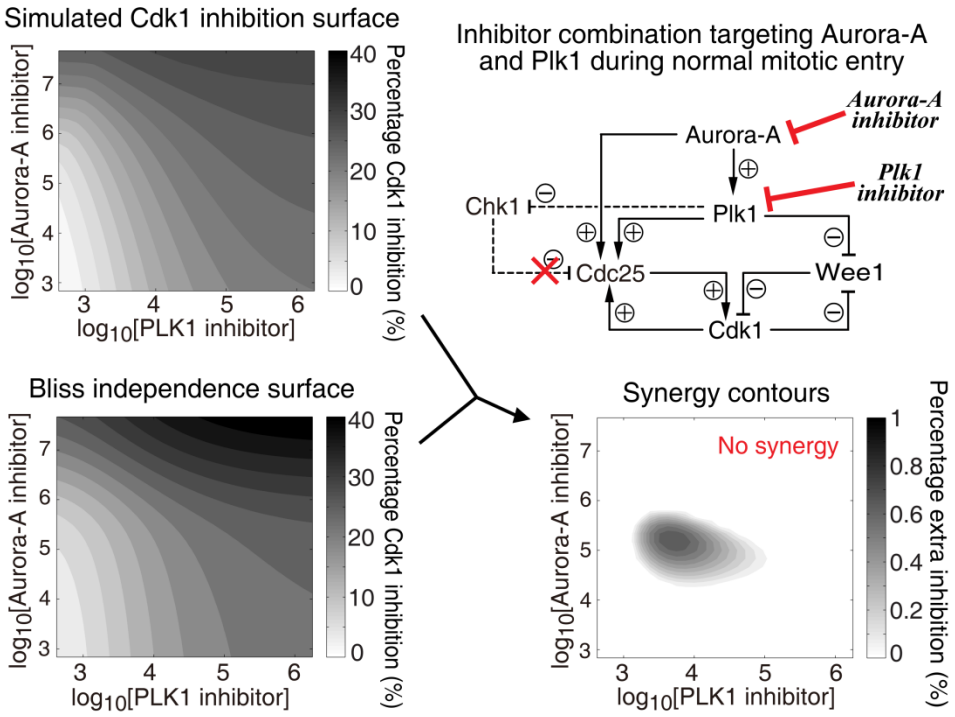

Fig. S6. Response surface simulation of combinational inhibition of Aurora-A and Plk1 during normal mitotic entry. There is no obvious synergistic combination effect (bottom right panel).

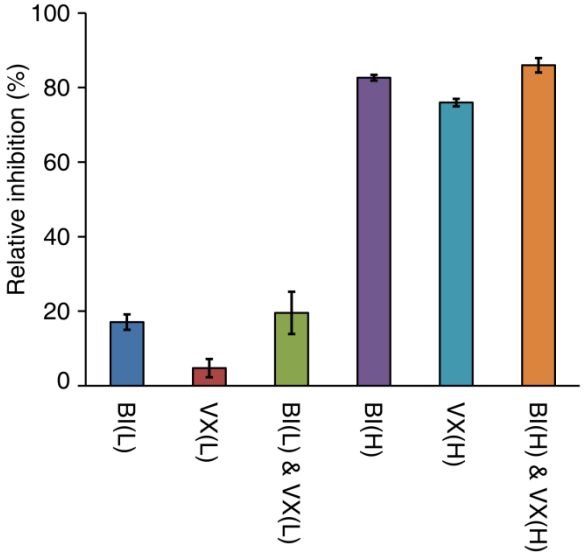

Fig. S7. Hela cells were treated with lower levels of VX-680 [VX(L), 3 nM] and BI-2536 [BI(L), 1 nM], and also were treated with higher levels of VX-680 [VX(H), 15 μM] and BI-2536 [BI(H), 5 μM]. The percentage of apoptotic and death cells was measured using Cell Counting Kit-8 assay. *n*=3 for each.